2015 IEEE International Conference on Robotics and Automation (ICRA)
Washington State Convention Center
Seattle, Washington, May 26-30, 2015

The free configuration space of a Kirchhoff elastic rod is path-connected

Andy Borum and Timothy Bretl

Abstract— **In this paper, we show that the free configuration space of a Kirchhoff elastic rod is path-connected. By free configuration space, we mean the set of all equilibrium configurations of the rod that are stable (i.e. locally minimize elastic potential energy) and do not experience self-intersections. We also provide semi-analytical expressions for paths in the free configuration space that connect any two stable equilibrium configurations that do not contain self-intersections. These results are applied to the problem of manipulation planning for deformable objects.**

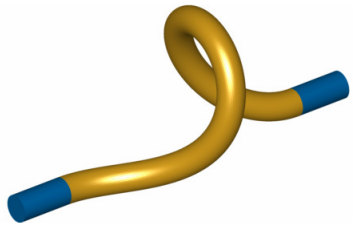

Fig. 1: An elastic rod (yellow) held at each end by a robotic gripper (blue).

I. INTRODUCTION

Consider a thin deformable wire or cable held at each end by a robotic gripper (Fig. 1). We call this deformable object an elastic rod. Static configurations of the rod that can be observed in experiments are those that locally minimize the elastic potential energy stored in the rod (i.e. are stable equilibrium configurations) and do not contain self-intersections. (See Fig. 3d for an example of a self-intersecting rod.) Given two such configurations, we are interested in finding a path of each gripper that causes the rod to move between the two configurations while avoiding self-collisions and remaining a stable equilibrium configuration throughout the motion. Equivalently, we may think of the problem as finding a path *of the rod* through the set of all non-self-intersecting stable equilibrium configurations. We call this set the free configuration space of the rod. In this paper, we prove that this set is path-connected so that such a path always exists. Furthermore, we provide a semi-analytical procedure for constructing the paths of the robotic grippers that produce the desired motion of the rod.

Manipulation planning in the set of equilibrium configurations of the rod was proposed in the seminal work of Lamiraux and Kavraki [1]. Rather than directly planning paths of the grippers holding the rod, this approach attempts to plan a path *of the rod* through its free configuration space. However, the procedure to derive the free configuration space was not clear at the time of their work. Bretl and McCarthy [2] later showed that the configuration space of the rod, i.e. the set of all equilibrium configurations (both stable and unstable), is a six-dimensional smooth manifold. They also provided a computational test to distinguish between stable and unstable equilibrium configurations, and a collision checking algorithm was used to find self-intersections. This allowed for a sampling-based planning algorithm to be used in which configurations of the rod could be sampled directly.

The work of Bretl and McCarthy [2], however, did not provide insight into the topological properties (such as path-connectedness) of the free configuration space, since the test to determine membership in this set was completely computational. Therefore, given starting and goal configurations of the rod, there was no guarantee that a feasible path of the rod in the free configuration space exists. Furthermore, the test for membership in the free configuration space was computationally expensive compared to sampling points in the configuration space, which adversely affected the computation time needed to find a feasible path.

We consider the configuration space derived by Bretl and McCarthy [2], which we denote by $\mathcal{A}$. Given a point $a \in \mathcal{A}$, the corresponding configuration of the rod is found by solving a system of ordinary differential equations using a as the initial condition. These differential equations are scale invariant [3], and we use this property to construct paths in the free configuration space of the rod connecting any two non-self-intersecting stable configurations. Our main result is that the free configuration space of the elastic rod is path-connected. Once we have found a path in the free configuration space, we can map the path of the rod to a path of the robotic grippers holding the ends of the rod. Compared to using a sampling-based algorithm, this approach guarantees that a feasible path will be found and allows us to bypass some of the computations needed to determine if sampled points are members of the free configuration space.

A qualitative description of our approach to planning in the free configuration space is described in Section II. The free configuration space of the rod is described in Section III. In Section IV, we show that the differential equations governing the rod's configuration are scale-invariant. We use this property in Section V to show that the set of non-self-intersecting stable configurations is path-connected. These results are applied to the manipulation planning problem in Section VI. Future work is discussed in Section VII.

*This work was supported by the NSF under Grant No. IIS-1320519. The work of A. Borum was supported by the NSF-GRFP under Grant No. DGE-1144245.

Andy Borum and Timothy Bretl are with the Department of Aerospace Engineering, University of Illinois at Urbana-Champaign, Urbana, IL, 61801, USA, {borum2,tbretl}@illinois.edu

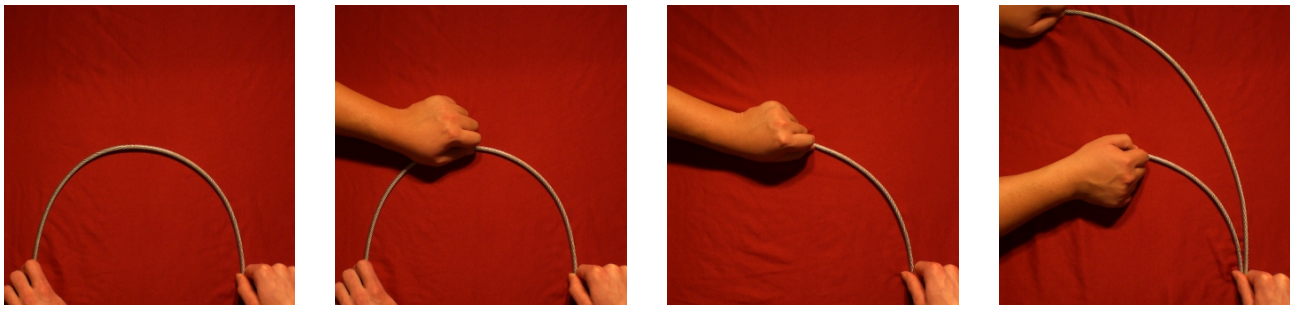

(a) (b) (c) (d)

Fig. 2: By cutting the rod in Fig. 2a in half and then scaling the shortened rod by a factor of two, as in Fig. 2d, a new configuration of the rod in Fig. 2a can be found. This gives a canonical way of "unbending" a deformed rod. These canonical deformations allow us to manipulate the rod between two non-self-intersecting stable equilibrium configurations.

II. A QUALITATIVE DESCRIPTION OF MANIPULATION

Before giving a mathematical description of the elastic rod, we provide a qualitative interpretation of our approach to the problem of manipulation planning. Our method relies on three properties of the rod. Here, we give arguments based on experimental images of an elastic rod and physical intuition. In later sections, we will mathematically prove these facts.

First, consider the elastic rod of unit length in Fig. 2a, and attach a coordinate frame to the right end of the rod (we will call the right end the base of the rod). Assume that this equilibrium configuration of the rod is stable and does not contain self-intersections (this is satisfied by the rod in Fig. 2a). Relative to the coordinate frame at the right end of the rod, let $r(t)$ with $t \in [0, 1]$ be an arc-length parameterized curve describing the shape of the rod. Now imagine that the rod is grasped at length $L = 1/2$ from the base of the rod, as in Fig. 2b, and then the remaining portion of the rod is removed, as in Fig. 2c. The first property that we emphasize is that the remaining portion of the rod, which has length $L = 1/2$, is stable and non-self-intersecting. This portion of the rod is described by the curve $r(t)$ with $t \in [0, 1/2]$.

Now consider a second elastic rod of unit length whose base is held in the same position and orientation as the rod of length $L = 1/2$. One possible equilibrium configuration of the longer rod, shown in Fig. 2d, is a scaling of the shorter rod. More specifically, the curve $2r(t/2) = r(Lt)/L$ with $t \in [0, 1]$ is an equilibrium configuration of the rod. Furthermore, we claim that this configuration is non-self-intersecting (which is clear from Fig. 2d) and is stable (which is not immediately obvious). This is the second property that we want to emphasize.

In this construction, the length $L = 1/2$ at which we grasped the rod could have been any positive fraction of the rod's length, i.e. the above arguments hold for any $L \in (0, 1]$. Now imagine that this process is repeated continuously, starting with the unit length rod in Fig. 2a, removing a small portion of the rod, and then rescaling the rod. As this process is executed, the shape of the rod is described by the curve $r(Lt)/L$, $t \in [0, 1]$, with L starting at 1 and continuously decreasing toward 0. This gives us a continuous deformation of the unit length rod, and as $L \to 0$, the unit length rod approaches the straight configuration. Therefore, this procedure gives us a canonical way of "untwisting" and "unbending" the rod, and if the initial configuration of the rod is stable and non-self-intersecting, every configuration along this canonical deformation is stable and non-self-intersecting.

Given any two non-self-intersecting stable equilibrium configurations of the rod, we can apply the above procedure to deform each rod arbitrarily close to the straight configuration, and therefore arbitrarily close to each other. The final property that we emphasize is that once the two rods are close enough to the straight configuration, either rod can be deformed into the other while remaining a stable equilibrium configuration and without intersecting itself. The concatenation of these three deformations (canonically "unbending" toward the straight shape, manipulating close to the straight shape, and then canonically bending into the new configuration) allows us to manipulate the rod between any two non-self-intersecting stable equilibrium configurations.

Once the three properties described in this section are accepted as true, this proves that the free configuration space of the elastic rod is path-connected, and the problem of manipulation becomes easy. In the remainder of the paper, we prove these three properties and answer the question "How close to the straight shape do two configurations need to be so that one can be deformed into the other?"

III. THE CONFIGURATION SPACE OF THE ROD

In this section, we show that each equilibrium configuration of a Kirchhoff elastic rod [4] corresponds to a unique point in $\mathbb{R}^6$. We also provide a computational test to determine if an equilibrium configuration is stable. The results in this section originally appeared in Bretl and McCarthy [2]. In their work, stable equilibrium configurations of a Kirchhoff elastic rod were formulated as local solutions of an optimal control problem on the Lie group $SE(3)$. We forgo describing this optimal control formulation and instead work directly with the differential equations that result from analyzing the optimal control problem.

We will assume, without loss of generality, that the rod has unit length. We will also assume that the rod is straight in the undeformed configuration. Using $t \in [0,1]$ to denote arc-length along the rod, the position and orientation of the rod at arc-length t are described by an element $q(t)$ of the special Euclidean group $SE(3)$. Thus, the shape of the rod is described by a continuous map $q\colon [0,1] \to SE(3)$. In the Kirchhoff elastic rod model, the rod is allowed to twist and bend, but is unshearable and inextensible [4]. Therefore, the map $q\colon [0,1] \to SE(3)$ must satisfy

$$\frac{dq}{dt} = q\left(u_1 X_1 + u_2 X_2 + u_3 X_3 + X_4\right) \tag{1}$$

for some $u\colon [0,1] \to \mathbb{R}^3$, where

$$X_1 = \begin{bmatrix} 0 & 0 & 0 & 0 \\ 0 & 0 & -1 & 0 \\ 0 & 1 & 0 & 0 \\ 0 & 0 & 0 & 0 \end{bmatrix} \quad X_2 = \begin{bmatrix} 0 & 0 & 1 & 0 \\ 0 & 0 & 0 & 0 \\ -1 & 0 & 0 & 0 \\ 0 & 0 & 0 & 0 \end{bmatrix} \quad X_3 = \begin{bmatrix} 0 & -1 & 0 & 0 \\ 1 & 0 & 0 & 0 \\ 0 & 0 & 0 & 0 \\ 0 & 0 & 0 & 0 \end{bmatrix}$$
$$X_4 = \begin{bmatrix} 0 & 0 & 0 & 1 \\ 0 & 0 & 0 & 0 \\ 0 & 0 & 0 & 0 \\ 0 & 0 & 0 & 0 \end{bmatrix} \quad X_5 = \begin{bmatrix} 0 & 0 & 0 & 0 \\ 0 & 0 & 0 & 1 \\ 0 & 0 & 0 & 0 \\ 0 & 0 & 0 & 0 \end{bmatrix} \quad X_6 = \begin{bmatrix} 0 & 0 & 0 & 0 \\ 0 & 0 & 0 & 0 \\ 0 & 0 & 0 & 1 \\ 0 & 0 & 0 & 0 \end{bmatrix}$$

is a basis for $\mathfrak{se}(3)$, the Lie algebra of $SE(3)$. The function $u_1\colon [0,1] \to \mathbb{R}$ is the twisting strain and the functions u_2 and $u_3\colon [0,1] \to \mathbb{R}$ are the bending strains along the rod.

Each end of the rod is held by a robotic gripper. We will assume, without loss of generality, that the base of the rod is held fixed at $q(0) = e$, where e is the identity element of $SE(3)$. This provides the initial condition for the differential equation (1). The gripper holding the rod at $t = 1$ is free to move in $SE(3)$. We now must find functions $u\colon [0,1] \to \mathbb{R}^3$ that produce equilibrium configurations of the rod.

Define the set $\mathcal{A} \subset \mathbb{R}^6$ by

$$\mathcal{A} = \{a \in \mathbb{R}^6 : (a_2, a_3, a_5, a_6) \neq (0,0,0,0)\} \tag{2}$$

The set $\mathcal{A}$ is simply $\mathbb{R}^6$ with a two-dimensional plane removed. Each point in $\mathcal{A}$ corresponds to an equilibrium configuration of the rod. This fact is proven in Theorem 5 of Bretl and McCarthy [2], and for path planning, $\mathcal{A}$ serves as the configuration space of the rod. We now outline the procedure for mapping points in $\mathcal{A}$ to rod configurations.

Given $a \in \mathcal{A}$, solve the six ordinary differential equations

$$\begin{aligned} \frac{d\mu_1}{dt} &= \frac{\mu_3\mu_2}{c_3} - \frac{\mu_2\mu_3}{c_2} & \frac{d\mu_4}{dt} &= \frac{\mu_3\mu_5}{c_3} - \frac{\mu_2\mu_6}{c_2} \\ \frac{d\mu_2}{dt} &= \mu_6 + \frac{\mu_1\mu_3}{c_1} - \frac{\mu_3\mu_1}{c_3} & \frac{d\mu_5}{dt} &= \frac{\mu_1\mu_6}{c_1} - \frac{\mu_3\mu_4}{c_3} \\ \frac{d\mu_3}{dt} &= -\mu_5 + \frac{\mu_2\mu_1}{c_2} - \frac{\mu_1\mu_2}{c_1} & \frac{d\mu_6}{dt} &= \frac{\mu_2\mu_4}{c_2} - \frac{\mu_1\mu_5}{c_1} \end{aligned} \tag{3}$$

on the interval $t \in [0,1]$ with the initial condition $\mu(0) = a$, where $c_1 > 0$ is the torsional stiffness of the rod and $c_2 > 0$ and $c_3 > 0$ are the bending stiffnesses of the rod. The resulting function $\mu\colon [0,1] \to \mathbb{R}^6$ can be interpreted as the vector of internal forces and torques along the rod [2].

Next, define $u\colon [0,1] \to \mathbb{R}^3$ by

$$u_i = \mu_i / c_i \quad \text{for } i = 1,2,3 \tag{4}$$

Solving (1) with this choice of u produces an equilibrium shape of the rod. We denote an equilibrium configuration by the pair of functions (q,u). Each (q,u) and the corresponding μ are completely defined by the choice of $a \in \mathcal{A}$. Denote the resulting maps by $(q,u) = \Psi(a)$ and $\mu = \Gamma(a)$, and define $\mathcal{C} = \Psi(\mathcal{A})$. In Theorem 5 of Bretl and McCarthy [2], it is shown that the map Ψ is injective, i.e. for each $(q,u) \in \mathcal{C}$ there exists a unique $a \in \mathcal{A}$ such that $(q,u) = \Psi(a)$.

Next, we need to determine which equilibrium configurations of the rod, i.e. which $a \in \mathcal{A}$, correspond to stable equilibrium configurations. Suppose $(q,u) = \Psi(a)$ and $\mu = \Gamma(a)$ for some $a \in \mathcal{A}$. For $w \in \mathbb{R}^6$, define the matrices

$$\mathbf{G} = \operatorname{diag}(c_1^{-1}, c_2^{-1}, c_3^{-1}, 0, 0, 0)$$

$$\mathbf{F}(w) = \begin{bmatrix} 0 & c_{32}w_3 & c_{32}w_2 & 0 & 0 & 0 \\ c_{13}w_3 & 0 & c_{13}w_1 & 0 & 0 & 1 \\ c_{21}w_2 & c_{21}w_1 & 0 & 0 & -1 & 0 \\ 0 & -c_2^{-1}w_6 & c_3^{-1}w_5 & 0 & c_3^{-1}w_3 & -c_2^{-1}w_2 \\ c_1^{-1}w_6 & 0 & -c_3^{-1}w_4 & -c_3^{-1}w_3 & 0 & c_1^{-1}w_1 \\ -c_1^{-1}w_5 & c_2^{-1}w_4 & 0 & c_2^{-1}w_2 & -c_1^{-1}w_1 & 0 \end{bmatrix}$$

$$\mathbf{H}(w) = \begin{bmatrix} 0 & c_3^{-1}w_3 & -c_2^{-1}w_2 & 0 & 0 & 0 \\ -c_3^{-1}w_3 & 0 & c_1^{-1}w_1 & 0 & 0 & 0 \\ c_2^{-1}w_2 & -c_1^{-1}w_1 & 0 & 0 & 0 & 0 \\ 0 & 0 & 0 & 0 & c_3^{-1}w_3 & -c_2^{-1}w_2 \\ 0 & 0 & 1 & -c_3^{-1}w_3 & 0 & c_1^{-1}w_1 \\ 0 & -1 & 0 & c_2^{-1}w_2 & -c_1^{-1}w_1 & 0 \end{bmatrix}$$

where $c_{ij} = c_i^{-1} - c_j^{-1}$ for $i,j = 1,2,3$. Now solve the linear, arc-length-varying matrix differential equations

$$\frac{d\mathbf{M}}{dt} = \mathbf{F}(\mu(t))\mathbf{M} \qquad \frac{d\mathbf{J}}{dt} = \mathbf{G}\mathbf{M} + \mathbf{H}(\mu(t))\mathbf{J} \tag{5}$$

with initial conditions $\mathbf{M}(0) = I$ and $\mathbf{J}(0) = 0$. Then, (q,u) is a stable equilibrium configuration if and only if $\det(\mathbf{J}(t)) \neq 0$ for all $t \in (0,1]$. This result is proven in Theorem 7 of Bretl and McCarthy [2]. The matrix functions $\mathbf{M}$ and $\mathbf{J}$ are both completely determined by the choice of $a \in \mathcal{A}$. Define this map by $(\mathbf{M}, \mathbf{J}) = \Lambda(a)$. A point $t \in (0,1]$ at which $\det(\mathbf{J}(t)) = 0$ is called a conjugate point. When we refer to conjugate points along the equilibrium configuration $(q,u) = \Psi(a)$, we mean arc-lengths $t \in (0,1]$ at which $\det(\mathbf{J}(t)) = 0$, where $(\mathbf{M}, \mathbf{J}) = \Lambda(a)$.

We can now determine which equilibrium configurations of the rod are stable. Denote the set of all $a \in \mathcal{A}$ that correspond to stable equilibrium configurations by $\mathcal{A}_{\text{stable}}$, and let $\mathcal{C}_{\text{stable}} = \Psi(\mathcal{A}_{\text{stable}})$. Also, define the map $\Phi : \mathcal{C} \to SE(3)$ by $(q,u) \mapsto q(1)$. Given a path of the rod in $\mathcal{C}_{\text{stable}}$, the function Φ can be used to find the path of the robotic gripper that causes the rod to follow the path in $\mathcal{C}_{\text{stable}}$.

Finally, we define $\mathcal{A}_{\text{free}} \subset \mathcal{A}_{\text{stable}}$ to be the set of all $a \in \mathcal{A}$ that correspond to stable equilibrium configurations of the rod that do not contain self-intersections. If there are no obstacles in the workspace of the rod, then we may think of $\mathcal{A}$ as the rod's configuration space and $\mathcal{A}_{\text{free}}$ as the free configuration space. Given two points a and $a' \in \mathcal{A}_{\text{free}}$, we would like to find a continuous path $\alpha\colon [0,1] \to \mathcal{A}_{\text{free}}$ such that $\alpha(0) = a$ and $\alpha(1) = a'$. The corresponding path of the rod is then given by $\Psi \circ \alpha$, and the path of the robotic gripper that causes the desired motion of the rod is $\Phi \circ \Psi \circ \alpha$.

One approach for constructing this path is to use a sampling-based planning algorithm [5]. The analysis we have done so far, however, does not guarantee that such

a path exists. Furthermore, when using this sampling-based approach, the matrix differential equations in (5) must be solved, the determinant of $\mathbf{J}(t)$ must be computed for all $t \in (0,1]$, and a collision checking algorithm must be evaluated at each point along the path in $\mathcal{A}$. This must be done to ensure the path remains in $\mathcal{A}_{\text{free}}$. In Section V, we will construct a path in $\mathcal{A}_{\text{free}}$ using an arbitrary path in $\mathcal{A}$ that connects the starting and goal configurations of the rod.

IV. SCALE INVARIANCE OF THE GOVERNING DIFFERENTIAL EQUATIONS

We will now establish a property of the differential equations (1), (3), and (5) known as scale invariance [3]. This property leads to scaling relationships between solutions of (1), (3), and (5). These scaling relationships will be used in Section V to show that $\mathcal{A}_{\text{free}}$ is path-connected.

Suppose $a \in \mathcal{A}_{\text{free}}$. Let

$$\mu = \Gamma(a) \quad (q,u) = \Psi(a) \quad (\mathbf{M},\mathbf{J}) = \Lambda(a)$$

Thus q solves (1), μ solves (3), and $\mathbf{M}$ and $\mathbf{J}$ solve (5) with the initial conditions $q(0) = e$, $\mu(0) = a$, $\mathbf{M}(0) = I$, and $\mathbf{J}(0) = 0$, and u is defined by (4). Next, let $L \in (0,1]$, and define the map $S_L \colon \mathbb{R}^6 \to \mathbb{R}^6$ by

$$S_L(w) = \begin{bmatrix} Lw_1 & Lw_2 & Lw_3 & L^2 w_4 & L^2 w_5 & L^2 w_6 \end{bmatrix}^T \quad (6)$$

for all $w \in \mathbb{R}^6$. Now let

$$\nu = \Gamma(S_L(a)) \quad (p,v) = \Psi(S_L(a)) \quad (\mathbf{N},\mathbf{K}) = \Lambda(S_L(a))$$

We have scaled the point a using S_L and evaluated the rod's configuration at this scaled value.

Now define the matrices D_L, M_L, and J_L by

$$\begin{aligned} D_L &= \text{diag}(1,1,1,L) \\ M_L &= \text{diag}(L,L,L,L^2,L^2,L^2) \\ J_L &= \text{diag}(1,1,1,L^{-1},L^{-1},L^{-1}) \end{aligned}$$

We claim that the following relations hold:

$$\nu(t) = S_L(\mu(Lt)) \quad (7)$$

$$v(t) = Lu(Lt) \quad (8)$$

$$p(t) = D_L q(Lt) D_L^{-1} \quad (9)$$

$$\mathbf{N}(t) = M_L \mathbf{M}(Lt) M_L^{-1} \quad \mathbf{K}(t) = J_L \mathbf{J}(Lt) M_L^{-1} \quad (10)$$

Equations (7)-(10) relate the configurations a and $S_L(a)$ of the rod through scaling relationships. Computations verifying these relations are presented in Appendix A.

These scaling relationships have three main implications.

- It is clear from (2) and (6) that since $a \in \mathcal{A}$ and $L \in (0,1]$, then $S_L(a) \in \mathcal{A}$ as well.
- We claim that $S_L(a) \in \mathcal{A}_{\text{stable}}$, i.e. (p,v) is a stable equilibrium configuration. From Section III, we know that (p,v) is a stable equilibrium configuration if and only if $\det(\mathbf{K}(t)) \neq 0$ for all $t \in (0,1]$. Now note that both J_L and M_L^{-1} are nonsingular. Therefore, from (10), $\mathbf{K}(t)$ is singular if and only if $\mathbf{J}(Lt)$ is singular. Since $a \in \mathcal{A}_{\text{stable}}$, we know that $\det(\mathbf{J}(t)) \neq 0$ for all $t \in (0,1]$. Finally, since $L \in (0,1]$, $\det(\mathbf{J}(Lt)) \neq 0$ for all $t \in (0,1]$. Thus $\det(\mathbf{K}(t)) \neq 0$ for all $t \in (0,1]$.
- We claim that $S_L(a) \in \mathcal{A}_{\text{free}}$, i.e. the configuration (p,v) does not contain self-intersections. Since q and p are maps taking values in $SE(3)$, we have

$$q(t) = \begin{bmatrix} R_q(t) & r_q(t) \\ 0 & 1 \end{bmatrix} \quad p(t) = \begin{bmatrix} R_p(t) & r_p(t) \\ 0 & 1 \end{bmatrix} \quad (11)$$

where $R_q(t)$ and $R_p(t) \in SO(3)$, and $r_q(t)$ and $r_p(t) \in \mathbb{R}^3$. Since $a \in \mathcal{A}_{\text{free}}$, the configuration (q,u) does not contain self-intersections, i.e. the map $r_q \colon [0,1] \to \mathbb{R}^3$ is injective. From (9), r_p and r_q are related by

$$r_p(t) = r_q(Lt)/L \quad (12)$$

Since $L \in (0,1]$, it is clear that r_p is injective. Therefore, (p,v) does not contain self-intersections.

We have shown that $S_L(a) \in \mathcal{A}_{\text{free}}$, and this holds for all $L \in (0,1]$. This produces a curve in $\mathcal{A}_{\text{free}}$, defined by $S_L(a)$ with $L \in (0,1]$, emanating from the origin in $\mathcal{A}$ (but not including the origin). Along this curve, we no longer need to perform the computations described at the end of Section III to ensure that we remain in $\mathcal{A}_{\text{free}}$. These curves will be used in the next section to show that $\mathcal{A}_{\text{free}}$ is path-connected.

V. TOPOLOGICAL PROPERTIES OF THE FREE CONFIGURATION SPACE

In Section IV, we derived analytical expressions for certain curves in $\mathcal{A}_{\text{free}}$. We will now show that any two of these curves can be connected with a third curve in $\mathcal{A}_{\text{free}}$. This will show that the set $\mathcal{A}_{\text{free}}$ is path-connected. We give a constructive procedure for finding this connecting curve; however, the procedure requires a numerical computation, and the curve is not defined in a closed-form expression.

Given a point $a \in \mathcal{A}_{\text{free}}$, we have established that $S_L(a) \in \mathcal{A}_{\text{free}}$ for all $L \in (0,1]$. We show the following two related facts in Appendices B and C, respectively:

- Given any $a \in \mathcal{A}$, there exists $L' \in (0,1]$ such that $S_L(a) \in \mathcal{A}_{\text{free}}$ for all $L \in (0,L']$.
- Let $\alpha \colon [0,1] \to \mathcal{A}$ be continuous. For each $s \in [0,1]$, choose $L'(s)$ such that $S_{L'(s)}(\alpha(s)) \in \mathcal{A}_{\text{free}}$ (this can be done using the above fact). Set

$$L^* = \inf\{L'(s) \colon s \in [0,1]\} > 0$$

Then $S_{L^*}(\alpha(s)) \in \mathcal{A}_{\text{free}}$ for all $s \in [0,1]$.

Given a path $\alpha \colon [0,1] \to \mathcal{A}$, we find L^* by performing two calculations. First, for each $s \in [0,1]$, compute $(\mathbf{M},\mathbf{J}) = \Lambda(\alpha(s))$. Let $t_1'(s)$ denote the first conjugate point along $\Psi(\alpha(s))$, i.e. the first point $t \in (0,1]$ at which $\det(\mathbf{J}(t)) = 0$. If $\det(\mathbf{J}(t)) \neq 0$ for all $t \in (0,1]$, set $t_1'(s) = 1$. Then let $0 < t_1 < \inf\{t_1'(s) \colon s \in [0,1]\}$. Next, for each $s \in [0,1]$, compute $(q,u) = \Psi(\alpha(s))$ and define r_q as in (11). Choose $t_2'(s)$ such that $r_q(t)$ is injective for all $t \in [0, t_2'(s)]$. After doing this for each $s \in [0,1]$, let $0 < t_2 < \inf\{t_2'(s) \colon s \in [0,1]\}$. Finally, choose $L^* = \min\{t_1, t_2\}$. It is shown in Appendix B that choosing L^* in this way satisfies $S_{L^*}(\alpha(s)) \in \mathcal{A}_{\text{free}}$ for all $s \in [0,1]$.

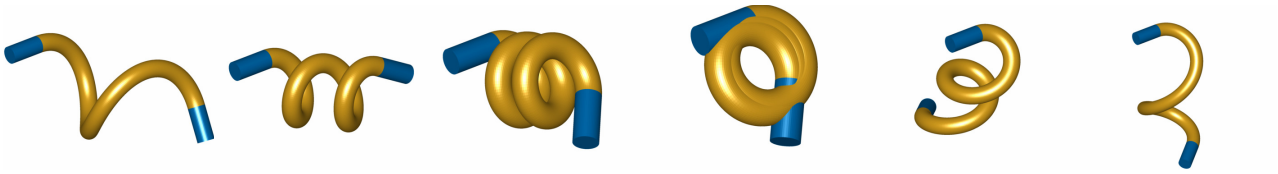

(a) (b) (c) (d) (e) (f)

Fig. 3: The path of the Kirchhoff elastic rod corresponding to the red path $\alpha\colon [0,1] \to \mathcal{A}$ in Figs. 4 and 5. Rods 3a and 3f are stable collision-free configurations. Rods 3b-3e are all unstable configurations, and rod 3d intersects itself.

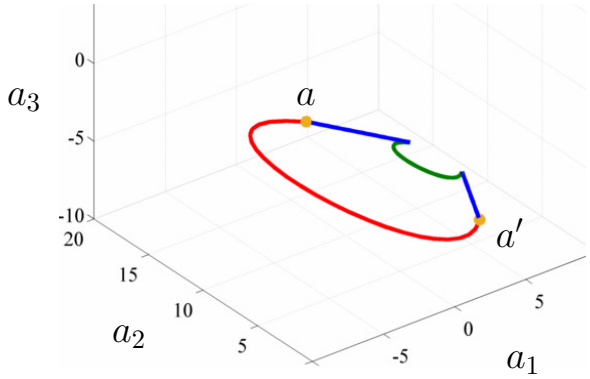

Fig. 4: The configuration space $\mathcal{A}$ projected onto the (a_1, a_2, a_3) axes. The red path corresponds to the rods in Fig. 3, and the blue and green paths correspond to the rods in Fig. 6.

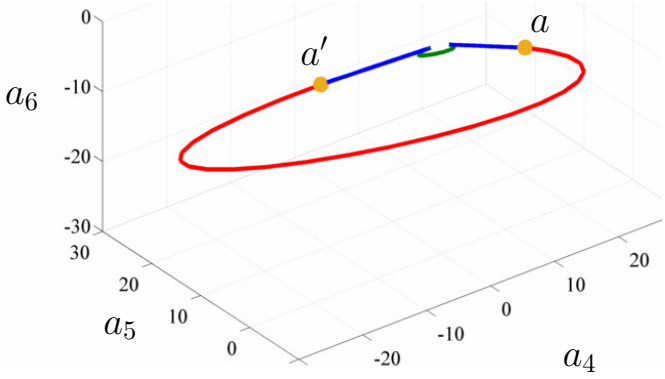

Fig. 5: The configuration space $\mathcal{A}$ projected onto the (a_4, a_5, a_6) axes. The red path corresponds to the rods in Fig. 3, and the blue and green paths correspond to the rods in Fig. 6.

We can now prove our main result.

Theorem 1: $\mathcal{A}_{\text{free}}$ is path-connected.

Proof: Let a and $a' \in \mathcal{A}_{\text{free}}$, and let $\alpha\colon [0,1] \to \mathcal{A}$ be a continuous path such that $\alpha(0) = a$ and $\alpha(1) = a'$. Such a path exists since $\mathcal{A}$ is path-connected. Choose L^* according to the above procedure so that $S_{L^*}(\alpha(s)) \in \mathcal{A}_{\text{free}}$ for all $s \in [0,1]$. Now consider the concatenation of the three paths

$$\begin{array}{ll} S_L(a) & \text{for } L \in [L^*, 1] \\ S_{L^*}(\alpha(s)) & \text{for } s \in [0,1] \\ S_L(a') & \text{for } L \in [L^*, 1] \end{array} \tag{13}$$

We have shown that these three paths are contained in $\mathcal{A}_{\text{free}}$. Since $S_{L^*}(a) = S_{L^*}(\alpha(0))$ and $S_{L^*}(a') = S_{L^*}(\alpha(1))$, these three paths are continuous. We have found a continuous path in $\mathcal{A}_{\text{free}}$ connecting a and a'. Our result follows. ■

By composing the path constructed in the proof with the functions Ψ and Φ, we can find a path of the robotic gripper that causes the rod to move from $\Psi(a)$ to $\Psi(a')$ while remaining in static equilibrium and avoiding self-collisions.

VI. APPLICATIONS TO MANIPULATION PLANNING FOR DEFORMABLE OBJECTS

In this section, we apply Theorem 1 to a simulated manipulation problem. Before showing this example, we note one important fact regarding self-intersections along the path constructed in Theorem 1. We stated that along this path, the rod does not intersect itself. This statement refers to the centerline of the rod. For any physical rod, the material comprising the rod will fill some radius δ around the centerline. Therefore, injectivity of the centerline does not necessarily guarantee the absence of self-collisions.

We can, however, quantify how close the centerline comes to a self-collision. Let $(q,u) = \Psi(a)$ for some $a \in \mathcal{A}_{\text{free}}$, define r_q as in (11), and let $\epsilon > 0$. Define δ_q by

$$\delta_q = \inf\{\|r_q(t_1) - r_q(t_2)\| \colon t_1, t_2 \in [0,1], |t_1 - t_2| \geq \epsilon\}$$

where $\|\cdot\|$ is the 2-norm. Then δ_q is the minimum distance between any two points on the rod (q,u) separated by an arc-length of at least ϵ. Now let $(p,v) = \Psi(S_L(a))$ for some $L \in (0,1]$ and define r_p as in (11). Using (12), we have

$$\begin{aligned} \delta_p &= \inf\{\|r_p(t_1) - r_p(t_2)\| \colon t_1, t_2 \in [0,1], |t_1 - t_2| \geq \epsilon\} \\ &= \inf\left\{ \frac{\|r_q(Lt_1) - r_q(Lt_2)\|}{L} \colon t_1, t_2 \in [0,1], |t_1 - t_2| \geq \epsilon \right\} \\ &\geq L^{-1} \inf\{\|r_q(t_1) - r_q(t_2)\| \colon t_1, t_2 \in [0,1], |t_1 - t_2| \geq \epsilon\} \\ &= L^{-1}\delta_q \end{aligned}$$

Therefore, the minimum distance δ_p between any two points on the rod (p,v) separated by an arc length of at least ϵ satisfies $\delta_p \geq L^{-1}\delta_q$. If we assume that the rod (q,u) does not self-intersect, i.e. $\delta_q > \delta$ (recall that δ is the radius of the rod), then the rod (p,v) does not self-intersect, since $L \in (0,1]$ and therefore $\delta_p \geq \delta_q > \delta$.

We now consider the example of manipulating a Kirchhoff elastic rod from the configuration (q,u) in Fig. 3a to the configuration (q',u') in Fig 3f. Both of these configurations are collision-free stable equilibrium configurations.

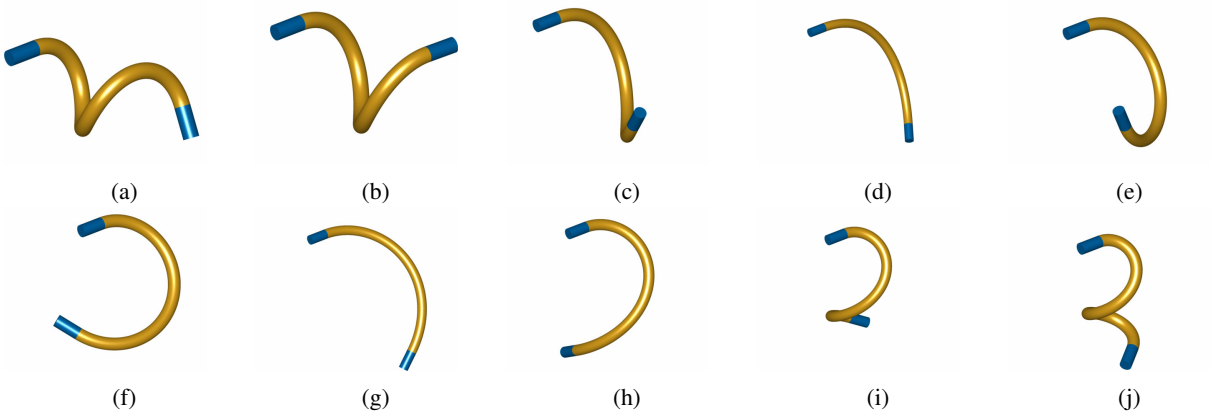

Fig. 6: The path of the Kirchhoff elastic rod corresponding to the blue and green paths in Figs. 4 and 5. Every configuration along this path is stable and does not contain self-collisions. Therefore, this is a path in the free configuration space. Note that rods 6a and 6j in this figure are identical to rods 3a and 3f in Fig. 3.

Therefore, there exist unique a and $a' \in \mathcal{A}_{\text{free}}$ such that $(q, u) = \Psi(a)$ and $(q', u') = \Psi(a')$. Before applying the result from Theorem 1, we will attempt to connect these two configurations with an arbitrarily chosen path in $\mathcal{A}$.

Fig. 4 shows a projection of the configuration space $\mathcal{A}$ onto the (a_1, a_2, a_3) axes, and Fig. 5 shows a projection onto the (a_4, a_5, a_6) axes. The two points a and a' are marked in each figure and are connected by a red path $\alpha\colon [0,1] \to \mathcal{A}$. The rod configurations shown in Fig. 3 correspond to points along this red path. The rod in Fig. 3d contains self-collisions, and the rods in Figs. 3b-3e are all unstable equilibrium configurations. Therefore, this path is not contained in $\mathcal{A}_{\text{free}}$.

We now apply Theorem 1 to find a path in $\mathcal{A}_{\text{free}}$ connecting a and a' using the path α. After performing the computations described in Section V to determine a suitable value of L^*, we find that $L^* = 0.3$ is sufficiently small, i.e. for each $s \in [0,1]$, the configuration $\Psi(\alpha(s))$ does not contain conjugate points or self-collisions for $t \in (0, L^*]$. The two curves $S_L(a)$ and $S_L(a')$ with $L \in [L^*, 1]$ are shown in blue in Figs. 4 and 5, and the curve $S_{L^*}(\alpha(s))$ with $s \in [0,1]$ is shown in green. From the proof of Theorem 1, we know that the concatenation of these three paths forms a continuous path in $\mathcal{A}_{\text{free}}$ connecting a and a'. The rod configurations in Fig. 6 correspond to points along this path in $\mathcal{A}_{\text{free}}$. As expected, all of these configurations are stable equilibrium configurations and do not contain self-intersections.

VII. CONCLUSIONS AND FUTURE WORK

We proved that the free configuration space of a Kirchhoff elastic rod is path-connected. This was shown by constructing paths in the free configuration space connecting any two collision-free stable equilibrium configurations. We applied these results to the problem of manipulation planning and found paths of the robotic grippers holding the ends of the rod that cause the rod to move between two stable equilibrium configurations while avoiding self-collisions.

Throughout the paper, we have ignored the possibility of having obstacles in the workspace of the rod, and such obstacles will often be present in applications. However, our results may be helpful when trying to find paths of the rod that do not collide with such obstacles. Suppose we have a path $\alpha\colon [0,1] \to \mathcal{A}_{\text{free}}$, where $\mathcal{A}_{\text{free}}$ now denotes the set of all stable equilibrium configurations that do not contain self-intersections and do not collide with the obstacles in the rod's workspace. Then, the two dimensional surface defined by $S_L(\alpha(s))$ with $s \in [0,1]$ and $L \in (0,1]$ contains only non-self-intersecting stable equilibrium configurations. Therefore, when moving along this surface, we only need to check that configurations do not collide with obstacles in order to ensure the configurations remain in $\mathcal{A}_{\text{free}}$. Searching on this surface is computationally inexpensive, but this limits us to a submanifold of the configuration space. We are then faced with the problem of deciding when we should leave this surface and begin searching on a new surface. This may be similar to the problem of deciding when to release and regrasp rigid objects during manipulation [6]. We leave the problem of manipulation with obstacles for future work.

APPENDIX A

In this appendix, we show that the relations (7)-(10) hold. Let $a \in \mathcal{A}$, $L \in (0,1]$, and $a' = S_L(a)$. Since $a = \mu(0)$, it is clear that $a' = \nu(0)$. We claim that $\nu\colon [0,1] \to \mathbb{R}^6$ is a solution of (3). To see this, consider the derivative of ν_1.

$$\begin{aligned}
\frac{d\nu_1(t)}{dt} &= \frac{d(L\mu_1(Lt))}{dt} = L^2 \frac{d(\mu_1(Lt))}{d(Lt)} \\
&= L^2 \left(\frac{\mu_3(Lt)\mu_2(Lt)}{c_3} - \frac{\mu_2(Lt)\mu_3(Lt)}{c_2} \right) \\
&= L^2 \left(L^{-2} \frac{\nu_3(t)\nu_2(t)}{c_3} - L^{-2} \frac{\nu_2(t)\nu_3(t)}{c_2} \right) \\
&= \frac{\nu_3(t)\nu_2(t)}{c_3} - \frac{\nu_2(t)\nu_3(t)}{c_2}
\end{aligned}$$

Similar computations show that ν_i satisfies (3) for $i = 2,3,4,5,6$. Each solution of (3) is completely determined by its initial condition. Thus, $\nu = \Gamma(\nu(0)) = \Gamma(a')$.

Next, using (4), we have

$$v_i(t) = c_i^{-1}\nu_i(t) = Lc_i^{-1}\mu_i(Lt) = Lu_i(Lt)$$

for $i = 1, 2, 3$. A direct computation shows that

$$D_L^{-1} X_i = X_i D_L^{-1} \qquad X_4 D_L^{-1} L = D_L^{-1} X_4$$

for $i = 1, 2, 3$. Now consider the derivative of $p(t)$.

$$\begin{aligned}
\frac{dp(t)}{dt} &= D_L \frac{dq(Lt)}{dt} D_L^{-1} = D_L \frac{dq(Lt)}{d(Lt)} D_L^{-1} L \\
&= D_L q(Lt) \left(\sum\nolimits_{i=1}^{3} u_i(Lt) X_i + X_4 \right) D_L^{-1} L \\
&= D_L q(Lt) D_L^{-1} \left(\sum\nolimits_{i=1}^{3} L u_i(Lt) X_i + X_4 \right) \\
&= p(t) \left(\sum\nolimits_{i=1}^{3} \nu_i(t) X_i + X_4 \right)
\end{aligned}$$

Also, we have $p(0) = D_L q(0) D_L^{-1} = D_L e D_L^{-1} = e$. Thus, p and v are the unique solutions of (4) and (1) corresponding to a'. Therefore, $(p, v) = \Psi(a')$.

Finally, consider the scaled matrices $\mathbf{N}$ and $\mathbf{K}$. Since $\mathbf{M}(0) = I$ and $\mathbf{J}(0) = 0$, it is clear that $\mathbf{N}(0) = I$ and $\mathbf{K}(0) = 0$. A direct computation shows that

$$\begin{aligned}
L M_L \mathbf{F}(w) M_L^{-1} &= \mathbf{F}(S_L(w)) \\
L J_L \mathbf{G} M_L^{-1} &= \mathbf{G} \\
L J_L \mathbf{H}(w) J_L^{-1} &= \mathbf{H}(S_L(w))
\end{aligned}$$

for all $w \in \mathbb{R}^6$. Using $\nu(t) = S_L(\mu(Lt))$, we have

$$\begin{aligned}
\frac{d\mathbf{N}(t)}{dt} &= M_L \frac{d\mathbf{M}(Lt)}{dt} M_L^{-1} = L M_L \frac{d\mathbf{M}(Lt)}{d(Lt)} M_L^{-1} \\
&= L M_L \mathbf{F}(\mu(Lt)) \mathbf{M}(Lt) M_L^{-1} \\
&= L M_L \mathbf{F}(\mu(Lt)) M_L^{-1} M_L \mathbf{M}(Lt) M_L^{-1} \\
&= \mathbf{F}(S_L(\mu(Lt))) \mathbf{N}(t) \\
&= \mathbf{F}(\nu(t)) \mathbf{N}(t)
\end{aligned}$$

A similar calculation shows that

$$\frac{d\mathbf{K}(t)}{dt} = \mathbf{G}\mathbf{N}(t) + \mathbf{H}(\nu(t)) \mathbf{K}(t)$$

APPENDIX B

In this appendix, we prove the following lemma.

Lemma 1: For any $a \in \mathcal{A}$, there exists L' such that $S_L(a) \in \mathcal{A}_{\text{free}}$ for all $L \in (0, L']$.

Before proving the lemma, we need to establish some facts about conjugate points along the configuration $\Psi(a)$.

Lemma 2: Let $(\mathbf{M}, \mathbf{J}) = \Lambda(a)$ for some $a \in \mathcal{A}$. Then there exists some $\epsilon > 0$ such that $\det(\mathbf{J}(t)) \neq 0$ for all $t \in (0, \epsilon]$, and the times at which $\det(\mathbf{J}(t)) = 0$ are isolated.

Proof: See Proposition 2.2 of Sachkov [7]. ■

We can now prove Lemma 1.

Proof: If $a \in \mathcal{A}_{\text{free}}$, then from Section IV we can choose $L' = 1$. Suppose $a \notin \mathcal{A}_{\text{free}}$. Then the configuration $\Psi(a)$ either contains conjugate points on the interval $t \in (0, 1]$, contains self-intersections, or both. We will assume that both occur, and this will take care of the other two cases.

Let $(\mathbf{M}, \mathbf{J}) = \Lambda(a)$. We assumed that there are conjugate points in the interval $(0, 1]$, i.e. points $t \in (0, 1]$ at which $\det(\mathbf{J}(t)) = 0$. From Lemma 2, we know that these points are positive and discrete, so there exists a smallest conjugate point. Denote this first conjugate point by t_1. Then $\det(\mathbf{J}(t)) \neq 0$ for all $t \in (0, t_1)$.

Now let $L \in (0, t_1)$. Then $Lt < t_1$ for all $t \in (0, 1]$. Thus, $\det(\mathbf{J}(Lt)) \neq 0$ for all $t \in (0, 1]$. Let $a' = S_L(a)$ and $(\mathbf{N}, \mathbf{K}) = \Lambda(a')$. We established in Section IV that $\mathbf{K}(t)$ is singular if and only if $\mathbf{J}(Lt)$ is singular. We conclude that $\det(\mathbf{K}(t)) \neq 0$ for all $t \in (0, 1]$, and therefore $a' \in \mathcal{A}_{\text{stable}}$.

Next, let $(q, u) = \Psi(a)$ and define r_q as in (11). We assumed that the configuration (q, u) contains self-collisions. Thus, r_q is not injective on the interval $t \in [0, 1]$. We claim that there exists $t_2 \in (0, 1]$ such that r_q is injective on the interval $t \in [0, t_2]$. To see this, recall that $q(0) = e$ and consider the derivative of q, given by (1), at $t = 0$.

$$\dot{q}(0) = \begin{bmatrix} 0 & -u_3 & u_2 & 1 \\ u_2 & 0 & -u_1 & 0 \\ -u_2 & u_1 & 0 & 0 \\ 0 & 0 & 0 & 0 \end{bmatrix}$$

Thus $\dot{r}_q(0) = [1 \ 0 \ 0]^T$, and there exists some short time interval $[0, t_2]$ along which r_q is injective. Now let $L \in (0, t_2)$, $(p, v) = \Psi(S_L(a))$, and define r_p as in (11). From (12), we see that r_p is injective for all $t \in [0, 1]$.

Now let $0 < L' < \min\{t_1, t_2\}$. Then for all $L \in (0, L']$, $\Psi(S_L(a))$ is non-self-intersecting and does not have conjugate points on the interval $t \in (0, 1]$, so $S_L(a) \in \mathcal{A}_{\text{free}}$. ■

APPENDIX C

In this appendix, we extend Lemma 1 in Appendix B to paths in $\mathcal{A}$. First, we need Lemma 3 to place a lower bound on conjugate times along paths in $\mathcal{A}$.

Lemma 3: If $\alpha \colon [0, 1] \to \mathcal{A}$ is continuous, then there exists $t_1 > 0$ such that the configuration $\Psi(\alpha(s))$ does not have conjugate points in the interval $(0, t_1]$ for all $s \in [0, 1]$.

Proof: See Proposition 2.6 of Sachkov [7]. ■

Lemma 4: Let $\alpha \colon [0, 1] \to \mathcal{A}$ be continuous. Then there exists $L^* > 0$ such that $S_{L^*}(\alpha(s)) \in \mathcal{A}_{\text{free}}$ for all $s \in [0, 1]$.

Proof: Choose t_1 according to Lemma 3. Then, for each $s \in [0, 1]$, choose $t'(s)$ so that the configuration $\Psi(\alpha(s))$ does not have self-intersections on the interval $(0, t'(s)]$. For each $s \in [0, 1]$, if $(q, u) = \Psi(\alpha(s))$ and r_q is defined by (11), then $\dot{r}_q(0) = [1 \ 0 \ 0]^T$, as we saw in the proof of Lemma 1. We can therefore choose $t_2 > 0$ such that $t'(s) > t_2$ for all $s \in [0, 1]$. Now let $L^* = \min\{t_1, t_2\} > 0$. ■

REFERENCES

[1] F. Lamiraux and L.E. Kavraki, Planning paths for elastic objects under manipulation constraints, *IJRR*, 20(3):188-208, 2001.

[2] T. Bretl and Z. McCarthy, Quasi-static manipulation of a Kirchhoff elastic rod based on a geometric analysis of equilibrium Configurations, *IJRR*, 33(1):48-68, 2014.

[3] P.J. Olver, *Applications of Lie Groups to Differential Equations*, Springer-Verlag, New York, 1993.

[4] S.S. Antman, *Nonlinear Problems of Elasticity*, Springer, New York, 2005.

[5] S.M. LaValle, *Planning Algorithms*, Cambridge University Press, New York, 2006.

[6] T. Siméon, J.-P. Laumond, J. Cortés, and A. Sahbani, Manipulation planning with probabilistic roadmaps, *IJRR*, 23(7-8):729-746, 2004.

[7] Y. Sachkov, Conjugate points in the Euler elastic problem, *JDCS*, 14(3):409-439, 2008.